
Deep Reinforcement Learning in Large Discrete Action Spaces

Gabriel Dulac-Arnold*, Richard Evans*, Hado van Hasselt, Peter Sunehag, Timothy Lillicrap, Jonathan Hunt, Timothy Mann, Theophane Weber, Thomas Degris, Ben Coppin

DULACARNOLD@GOOGLE.COM

Google DeepMind

Abstract

Being able to reason in an environment with a large number of discrete actions is essential to bringing reinforcement learning to a larger class of problems. Recommender systems, industrial plants and language models are only some of the many real-world tasks involving large numbers of discrete actions for which current methods are difficult or even often impossible to apply.

An ability to generalize over the set of actions as well as sub-linear complexity relative to the size of the set are both necessary to handle such tasks. Current approaches are not able to provide both of these, which motivates the work in this paper. Our proposed approach leverages prior information about the actions to embed them in a continuous space upon which it can generalize. Additionally, approximate nearest-neighbor methods allow for logarithmic-time lookup complexity relative to the number of actions, which is necessary for time-wise tractable training. This combined approach allows reinforcement learning methods to be applied to large-scale learning problems previously intractable with current methods. We demonstrate our algorithm’s abilities on a series of tasks having up to one million actions.

1. Introduction

Advanced AI systems will likely need to reason with a large number of possible actions at every step. Recommender systems used in large systems such as YouTube and Amazon must reason about hundreds of millions of items every second, and control systems for large industrial processes may have millions of possible actions that can be applied at every time step. All of these systems are fundamentally

*Equal contribution.

reinforcement learning (Sutton & Barto, 1998) problems, but current algorithms are difficult or impossible to apply.

In this paper, we present a new policy architecture which operates efficiently with a large number of actions. We achieve this by leveraging prior information about the actions to embed them in a continuous space upon which the actor can generalize. This embedding also allows the policy’s complexity to be decoupled from the cardinality of our action set. Our policy produces a continuous action within this space, and then uses an approximate nearest-neighbor search to find the set of closest discrete actions in logarithmic time. We can either apply the closest action in this set directly to the environment, or fine-tune this selection by selecting the highest valued action in this set relative to a cost function. This approach allows for generalization over the action set in logarithmic time, which is necessary for making both learning and acting tractable in time.

We begin by describing our problem space and then detail our policy architecture, demonstrating how we can train it using policy gradient methods in an actor-critic framework. We demonstrate the effectiveness of our policy on various tasks with up to one million actions, but with the intent that our approach could scale well beyond millions of actions.

2. Definitions

We consider a Markov Decision Process (MDP) where \mathcal{A} is the set of discrete actions, \mathcal{S} is the set of discrete states, $\mathcal{P} : \mathcal{S} \times \mathcal{A} \times \mathcal{S} \rightarrow \mathbb{R}$ is the transition probability distribution, $R : \mathcal{S} \times \mathcal{A} \rightarrow \mathbb{R}$ is the reward function, and $\gamma \in [0, 1]$ is a discount factor for future rewards. Each action $\mathbf{a} \in \mathcal{A}$ corresponds to an n -dimensional vector, such that $\mathbf{a} \in \mathbb{R}^n$. This vector provides information related to the action. In the same manner, each state $\mathbf{s} \in \mathcal{S}$ is a vector $\mathbf{s} \in \mathbb{R}^m$.

The return of an episode in the MDP is the discounted sum of rewards received by the agent during that episode: $R_t = \sum_{i=t}^T \gamma^{i-t} r(\mathbf{s}_i, \mathbf{a}_i)$. The goal of RL is to learn a policy $\pi : \mathcal{S} \rightarrow \mathcal{A}$ which maximizes the expected return over all episodes, $\mathbb{E}[R_1]$. The state-action value function $Q^\pi(\mathbf{s}, \mathbf{a}) = \mathbb{E}[R_1 | \mathbf{s}_1 = \mathbf{s}, \mathbf{a}_1 = \mathbf{a}, \pi]$ is the expected re-

turn starting from a given state \mathbf{s} and taking an action \mathbf{a} , following π thereafter. Q^π can be expressed in a recursive manner using the Bellman equation:

$$Q^\pi(\mathbf{s}, \mathbf{a}) = r(\mathbf{s}, \mathbf{a}) + \gamma \sum_{\mathbf{s}'} P(\mathbf{s}' | \mathbf{s}, \mathbf{a}) Q^\pi(\mathbf{s}', \pi(\mathbf{s}')).$$

In this paper, both Q and π are approximated by parametrized functions.

3. Problem Description

There are two primary families of policies often used in RL systems: value-based, and actor-based policies.

For value-based policies, the policy’s decisions are directly conditioned on the value function. One of the more common examples is a policy that is greedy relative to the value function:

$$\pi_Q(\mathbf{s}) = \arg \max_{\mathbf{a} \in \mathcal{A}} Q(\mathbf{s}, \mathbf{a}). \quad (1)$$

In the common case that the value function is a parameterized function which takes both state and action as input, $|\mathcal{A}|$ evaluations are necessary to choose an action. This quickly becomes intractable, especially if the parameterized function is costly to evaluate, as is the case with deep neural networks. This approach does, however, have the desirable property of being capable of generalizing over actions when using a smooth function approximator. If \mathbf{a}_i and \mathbf{a}_j are similar, learning about \mathbf{a}_i will also inform us about \mathbf{a}_j . Not only does this make learning more efficient, it also allows value-based policies to use the action features to reason about previously unseen actions. Unfortunately, execution complexity grows linearly with $|\mathcal{A}|$ which renders this approach intractable when the number of actions grows significantly.

In a standard actor-critic approach, the policy is explicitly defined by a parameterized actor function: $\pi_\theta : \mathcal{S} \rightarrow \mathcal{A}$. In practice π_θ is often a classifier-like function approximator, which scale linearly in relation to the number of actions. However, actor-based architectures avoid the computational cost of evaluating a likely costly Q-function on every action in the $\arg \max$ in Equation (1). Nevertheless, actor-based approaches do not generalize over the action space as naturally as value-based approaches, and cannot extend to previously unseen actions.

Sub-linear complexity relative to the action space and an ability to generalize over actions are both necessary to handle the tasks we interest ourselves with. Current approaches are not able to provide both of these, which motivates the approach described in this paper.

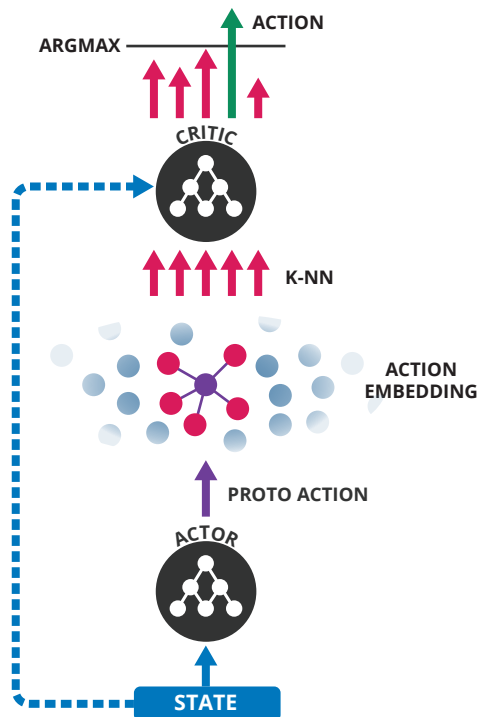


Figure 1. Wolpertinger Architecture

4. Proposed Approach

We propose a new policy architecture which we call the Wolpertinger architecture. This architecture avoids the heavy cost of evaluating all actions while retaining generalization over actions. This policy builds upon the actor-critic (Sutton & Barto, 1998) framework. We define both an efficient action-generating actor, and utilize the critic to refine our actor’s choices for the full policy. We use multi-layer neural networks as function approximators for both our actor and critic functions. We train this policy using Deep Deterministic Policy Gradient (Lillicrap et al., 2015).

The Wolpertinger policy’s algorithm is described fully in Algorithm 1 and illustrated in Figure 1. We will detail these in the following sections.

Algorithm 1 Wolpertinger Policy

State \mathbf{s} previously received from environment.
 $\hat{\mathbf{a}} = f_{\theta\pi}(\mathbf{s})$ {Receive proto-action from actor.}
 $\mathcal{A}_k = g_k(\hat{\mathbf{a}})$ {Retrieve k approximately closest actions.}
 $\mathbf{a} = \arg \max_{\mathbf{a}_j \in \mathcal{A}_k} Q_{\theta Q}(\mathbf{s}, \mathbf{a}_j)$
 Apply \mathbf{a} to environment; receive r, \mathbf{s}' .

4.1. Action Generation

Our architecture reasons over actions within a continuous space \mathbb{R}^n , and then maps this output to the discrete action

set \mathcal{A} . We will first define:

$$\begin{aligned} f_{\theta^\pi} : \mathcal{S} &\rightarrow \mathbb{R}^n \\ f_{\theta^\pi}(\mathbf{s}) &= \hat{\mathbf{a}}. \end{aligned}$$

f_{θ^π} is a function parametrized by θ^π , mapping from the state representation space \mathbb{R}^m to the action representation space \mathbb{R}^n . This function provides a proto-action in \mathbb{R}^n for a given state, which will likely not be a valid action, i.e. it is likely that $\hat{\mathbf{a}} \notin \mathcal{A}$. Therefore, we need to be able to map from $\hat{\mathbf{a}}$ to an element in \mathcal{A} . We can do this with:

$$\begin{aligned} g : \mathbb{R}^n &\rightarrow \mathcal{A} \\ g_k(\hat{\mathbf{a}}) &= \arg \min_{\mathbf{a} \in \mathcal{A}}^k \|\mathbf{a} - \hat{\mathbf{a}}\|_2. \end{aligned}$$

g_k is a k -nearest-neighbor mapping from a continuous space to a discrete set¹. It returns the k actions in \mathcal{A} that are closest to $\hat{\mathbf{a}}$ by L_2 distance. In the exact case, this lookup is of the same complexity as the $\arg \max$ in the value-function derived policies described in Section 3, but each step of evaluation is an L_2 distance instead of a full value-function evaluation. This task has been extensively studied in the approximate nearest neighbor literature, and the lookup can be performed in an approximate manner in logarithmic time (Muja & Lowe, 2014). This step is described by the bottom half of Figure 1, where we can see the actor network producing a proto-action, and the k -nearest neighbors being chosen from the action embedding.

4.2. Action Refinement

Depending on how well the action representation is structured, actions with a low Q -value may occasionally sit closest to $\hat{\mathbf{a}}$ even in a part of the space where most actions have a high Q -value. Additionally, certain actions may be near each other in the action embedding space, but in certain states they must be distinguished as one has a particularly low long-term value relative to its neighbors. In both of these cases, simply selecting the closest element to $\hat{\mathbf{a}}$ from the set of actions generated previously is not ideal.

To avoid picking these outlier actions, and to generally improve the finally emitted action, the second phase of the algorithm, which is described by the top part of Figure 1, refines the choice of action by selecting the highest-scoring action according to Q_{θ^Q} :

$$\pi_\theta(\mathbf{s}) = \arg \max_{\mathbf{a} \in g_k \circ f_{\theta^\pi}(\mathbf{s})} Q_{\theta^Q}(\mathbf{s}, \mathbf{a}). \quad (2)$$

This equation is described more explicitly in Algorithm 1. It introduces π_θ which is the full Wolpertinger policy. The parameter θ represents both the parameters of the action generation element in θ^π and of the critic in θ^Q .

¹For $k = 1$ this is a simple nearest neighbor lookup.

As we demonstrate in Section 7, this second pass makes our algorithm significantly more robust to imperfections in the choice of action representation, and is essential in making our system learn in certain domains. The size of the generated action set, k , is task specific, and allows for an explicit trade-off between policy quality and speed.

4.3. Training with Policy Gradient

Although the architecture of our policy is not fully differentiable, we argue that we can nevertheless train our policy by following the policy gradient of f_{θ^π} . We will first consider the training of a simpler policy, one defined only as $\tilde{\pi}_\theta = g \circ f_{\theta^\pi}$. In this initial case we can consider that the policy is f_{θ^π} and that the effects of g are a deterministic aspect of the environment. This allows us to maintain a standard policy gradient approach to train f_{θ^π} on *its* output $\hat{\mathbf{a}}$, effectively interpreting the effects of g as environmental dynamics. Similarly, the $\arg \max$ operation in Equation (2) can be seen as introducing a non-stationary aspect to the environmental dynamics.

4.4. Wolpertinger Training

The training algorithm’s goal is to find a parameterized policy π_{θ^*} which maximizes its expected return over the episode’s length. To do this, we find a parametrization θ^* of our policy which maximizes its expected return over an episode: $\theta^* = \arg \max_\theta \mathbb{E}[R_1 | \pi_\theta]$.

We perform this optimization using Deep Deterministic Policy Gradient (DDPG) (Lillicrap et al., 2015) to train both f_{θ^π} and Q_{θ^Q} . DDPG draws from two stability-inducing aspects of Deep Q-Networks (Mnih et al., 2015) to extend Deterministic Policy Gradient (Silver et al., 2014) to neural network function approximators by introducing a replay buffer (Lin, 1992) and target networks. DPG is similar to work introduced by NFQCA (Hafner & Riedmiller, 2011) and leverages the gradient-update originally introduced by ADHDP (Prokhorov et al., 1997).

The goal of these algorithms is to perform policy iteration by alternatively performing policy evaluation on the current policy with Q-learning, and then improving upon the current policy by following the policy gradient.

The critic is trained from samples stored in a replay buffer (Mnih et al., 2015). Actions stored in the replay buffer are generated by π_{θ^π} , but the policy gradient $\nabla_{\mathbf{a}} Q_{\theta^Q}(\mathbf{s}, \mathbf{a})$ is taken at $\hat{\mathbf{a}} = f_{\theta^\pi}(\mathbf{s})$. This allows the learning algorithm to leverage the otherwise ignored information of which action was actually executed for training the critic, while taking the policy gradient at the actual output of f_{θ^π} . The target action in the Q-update is generated by the full policy π_θ and not simply f_{θ^π} .

A detailed description of the algorithm is available in the

supplementary material.

5. Analysis

Time-complexity of the above algorithm scales linearly in the number of selected actions, k . We will see that in practice though, increasing k beyond a certain limit does not provide increased performance. There is a diminishing returns aspect to our approach that provides significant performance gains for the initial increases in k , but quickly renders additional performance gains marginal.

Consider the following simplified scenario. For a random proto-action \hat{a} , each nearby action has a probability p of being a bad or broken action with a low value of $Q(s, \hat{a}) - c$. The values of the remaining actions are uniformly drawn from the interval $[Q(s, \hat{a}) - b, Q(s, \hat{a}) + b]$, where $b \leq c$. The probability distribution for the value of a chosen action is therefore the mixture of these two distributions.

Lemma 1. *Denote the closest k actions as integers $\{1, \dots, k\}$. Then in the scenario as described above, the expected value of the maximum of the k closest actions is*

$$\mathbb{E} \left[\max_{i \in \{1, \dots, k\}} Q(s, i) \mid s, \hat{a} \right] = Q(s, a) + b - p^k(c - b) - \frac{2b}{k+1} \frac{1 - p^{k+1}}{1 - p}$$

The highest value an action can have is $Q(s, \hat{a}) + b$. The best action within the k -sized set is thus, in expectation, $p^k(c - b) + \frac{2b}{k+1} \frac{1 - p^{k+1}}{1 - p}$ smaller than this value.

The first term is in $O(p^k)$ and decreases exponentially with k . The second term is in $O(\frac{1}{k+1})$. Both terms decrease a relatively large amount for each additional action while k is small, but the marginal returns quickly diminish as k grows larger. This property is also observable in experiments in Section 7, notably in Figures 6 & 7. Using 5% or 10% of the maximal number of actions the performance is similar to when the full action set is used. Using the remaining actions would result in relatively small performance benefits while increasing computational time by an order of magnitude.

The proof to Lemma 1 is available in the supplementary material.

6. Related Work

There has been limited attention in the literature with regards to large discrete action spaces within RL. Most prior work has been concentrated on factorizing the action space into binary subspaces. Generalized value functions were proposed in the form of H-value functions (Pazis & Parr, 2011), which allow for a policy to evaluate $\log(|\mathcal{A}|)$ bi-

nary decisions to act. This learns a factorized value function from which a greedy policy can be derived for each subspace. This amounts to performing $\log(|\mathcal{A}|)$ binary operations on each action-selection step.

A similar approach was proposed which leverages Error-Correcting Output Code classifiers (ECOCs) (Dietterich & Bakiri, 1995) to factorize the policy’s action space and allow for parallel training of a sub-policy for each action subspace (Dulac-Arnold et al., 2012). In the ECOC-based approach case, a policy is learned through Rollouts Classification Policy Iteration (Lagoudakis & Parr, 2003), and the policy is defined as a multi-class ECOC classifier. Thus, the policy directly predicts a binary action code, and then a nearest-neighbor lookup is performed according to Hamming distance.

Both these approaches effectively factorize the action space into $\log(|\mathcal{A}|)$ binary subspaces, and then reason about these subspaces independently. These approaches can scale to very large action spaces, however, they require a binary code representation of each action, which is difficult to design properly. Additionally, the generalized value-function approach uses a Linear Program and explicitly stores the value function per state, which prevents it from generalizing over a continuous state space. The ECOC-based approach only defines an action producing policy and does not allow for refinement with a Q-function.

These approaches cannot naturally deal with discrete actions that have associated continuous representations. The closest approach in the literature uses a continuous-action policy gradient method to learn a policy in a continuous action space, and then apply the nearest discrete action (Van Hasselt et al., 2009). This is in principle similar to our approach, but was only tested on small problems with a uni-dimensional continuous action space (at most 21 discrete actions) and a low-dimensional observation space. In such small discrete action spaces, selecting the nearest discrete action may be sufficient, but we show in Section 7 that a more complex action-selection scheme is necessary to scale to larger domains.

Recent work extends Deep Q-Networks to ‘unbounded’ action spaces (He et al., 2015), effectively generating action representations for any action the environment provides, and picking the action that provides the highest Q. However, in this setup, the environment only ever provides a small (2-4) number of actions that need to be evaluated, hence they do not have to explicitly pick an action from a large set.

This policy architecture has also been leveraged by the authors for learning to attend to actions in MDPs which take in multiple actions at each state (Slate MDPs) (Sunehag et al., 2015).

7. Experiments

We evaluate the Wolpertinger agent on three environment classes: Discretized Continuous Control, Multi-Step Planning, and Recommender Systems. These are outlined below:

7.1. Discretized Continuous Environments

To evaluate how the agent’s performance and learning speed relate to the number of discrete actions we use the MuJoCo (Todorov et al., 2012) physics simulator to simulate the classic continuous control tasks cart-pole (). Each dimension d in the original continuous control action space is discretized into i equally spaced values, yielding a discrete action space with $|\mathcal{A}| = i^d$ actions.

In cart-pole swing-up, the agent must balance a pole attached to a cart by applying force to the cart. The pole and cart start in a random downward position, and a reward of +1 is received if the pole is within 5 degrees of vertical and the cart is in the middle 10% of the track, otherwise a reward of zero is received. The current state is the position and velocity of the cart and pole as well as the length of the pole. The environment is reset after 500 steps.

We use this environment as a demonstration both that our agent is able to reason with both a small and large number of actions efficiently, especially when the action representation is well-formed. In these tasks, actions are represented by the force to be applied on each dimension. In the cart-pole case, this is along a single dimension, so actions are represented by a single number.

7.2. Multi-Step Plan Environment

Choosing amongst all possible n -step plans is a general large action problem. For example, if an environment has i actions available at each time step and an agent needs to plan n time steps into the future then the number of actions i^n is quickly intractable for arg max-based approaches. We implement a version of this task on a puddle world environment, which is a grid world with four cell types: empty, puddle, start or goal. The agent consistently starts in the start square, and a reward of -1 is given for visiting an empty square, a reward of -3 is given for visiting a puddle square, and a reward of 250 is given and the episode ends if on a goal cell. The agent observes a fixed-size square window surrounding its current position.

The goal of the agent is to find the shortest path to the goal that trades off the cost of puddles with distance traveled. The goal is always placed in the bottom right hand corner of the environment and the base actions are restricted to moving right or down to guarantee goal discovery with random exploration. The action set is the set of all pos-

sible n -length action sequences. We have 2 base actions: {down, right}. This means that environments with a plan of length n have 2^n actions in total, for $n = 20$ we have $2^{20} \approx 1e6$ actions.

This environment demonstrates our agent’s abilities with very large number of actions that are more difficult to discern from their representation, and have less obvious continuity with regards to their effect on the environment compared to the MuJoCo tasks. We represent each action with the concatenation of each step of the plan. There are two possible steps which we represent as either $\{0, 1\}$ or $\{1, 0\}$. This means that a full plan will be a vector of concatenated steps, with a total length of $2n$. This representation was chosen arbitrarily, but we show that our algorithm is nevertheless able to reason well with it.

7.3. Recommender Environment

To demonstrate how the agent would perform on a real-world large action space problem we constructed a simulated recommendation system utilizing data from a live large-scale recommendation engine. This environment is characterized by a set of items to recommend, which correspond to the action set \mathcal{A} and a transition probability matrix W , such that $W_{i,j}$ defines the probability that a user will accept recommendation j given that the last item they accepted was item i . Each item also has a reward r associated with it if accepted by the user. The current state is the item the user is currently consuming, and the previously recommended items do not affect the current transition.

At each time-step, the agent presents an item i to the user with action \mathcal{A}_i . The recommended item is then either accepted by the user (according to the transition probability matrix) or the user selects a random item instead. If the presented item is accepted then the episode ends with probability 0.1, if the item is not accepted then the episode ends with probability 0.2. This has the effect of simulating user patience - the user is more likely to finish their session if they have to search for an item rather than selecting a recommendation. After each episode the environment is reset by selecting a random item as the initial environment state.

7.4. Evaluation

For each environment, we vary the number of nearest neighbors k from $k = 1$, which effectively ignores the re-ranking step described in Section 4.2, to $k = |\mathcal{A}|$, which effectively ignores the action generation step described in Section 4.1. For $k = 1$, we demonstrate the performance of the nearest-neighbor element of our policy $g \circ f_{\theta\pi}$. This is the fastest policy configuration, but as we see in the section, is not always sufficiently expressive. For $k = |\mathcal{A}|$, we demonstrate the performance of a policy that is greedy relative to Q , always choosing the true maximizing action

from \mathcal{A} . This gives us an upper bound on performance, but we will soon see that this approach is often computationally intractable. Intermediate values of k are evaluated to demonstrate the performance gains of partial re-ranking.

We also evaluate the performance in terms of training time and average reward for full nearest-neighbor search, and three approximate nearest neighbor configurations. We use FLANN (Muja & Lowe, 2014) with three settings we refer to as ‘Slow’, ‘Medium’ and ‘Fast’. ‘Slow’ uses a hierarchical k-means tree with a branching factor of 16, which corresponds to 99% retrieval accuracy on the recommender task. ‘Medium’ corresponds to a randomized K-d tree where 39 nearest neighbors at the leaf nodes are checked. This corresponds to a 90% retrieval accuracy in the recommender task. ‘Fast’ corresponds to a randomized K-d tree with 1 nearest neighbor at the leaf node checked. This corresponds to a 70% retrieval accuracy in the recommender task. These settings were obtained with FLANN’s auto-tune mechanism.

8. Results

In this section we analyze results from our experiments with the environments described above.

8.1. Cart-Pole

The cart-pole task was generated with a discretization of one million actions. On this task, our algorithm is able to find optimal policies. We have a video available of our final policy with one million actions, $k = 1$, and ‘fast’ FLANN lookup here: <http://goo.gl/3YFyAE>.

We visualize performance of our agent on a one million action cart-pole task with $k = 1$ and $k = 0.5\%$ in Figure 2, using an exact lookup. In the relatively simple cart-pole task the $k = 1$ agent is able to converge to a good policy. However, for $k = 0.5\%$, which equates to 5,000 actions, training has failed to attain more than 100,000 steps in the same amount of time.

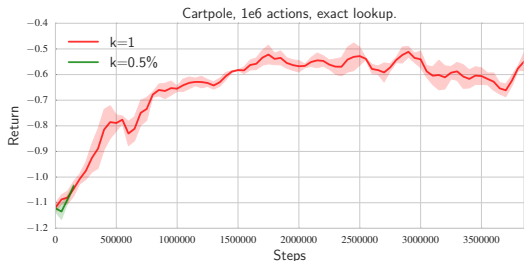


Figure 2. Agent performance for various settings of k with exact lookup as a function of steps. With 0.5% of neighbors, training time is prohibitively slow and convergence is not achieved.

Figure 3 shows performance as a function of wall-time on the cart-pole task. It presents the performance of agents with varying neighbor sizes and FLANN settings after the same number of seconds of training. Agents with $k = 1$ are able to achieve convergence after 150,000 seconds whereas $k = 5,000$ (0.5% of actions) trains much more slowly.

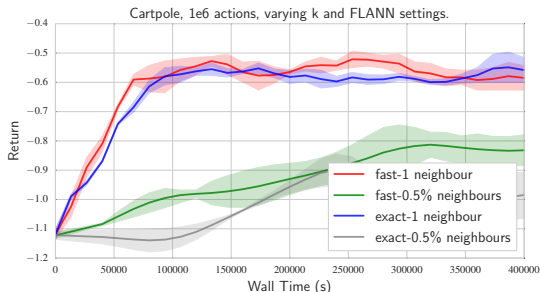


Figure 3. Agent performance for various settings of k and FLANN as a function of wall-time on one million action cart-pole. We can see that with 0.5% of neighbors, training time is prohibitively slow.

# Neighbors	Exact	Slow	Medium	Fast
1	18	2.4	8.5	23
0.5% – 5,000	0.6	0.6	0.7	0.7

Table 1. Median steps/second as a function of k & FLANN settings on cart-pole.

Table 1 display the median steps per second for the training algorithm. We can see that FLANN is only helpful for $k = 1$ lookups. Once $k = 5,000$, all the computation time is spent on evaluating Q instead of finding nearest neighbors. FLANN performance impacts nearest-neighbor lookup negatively for all settings except ‘fast’ as we are looking for a nearest neighbor in a single dimension. We will see in the next section that for more action dimensions this is no longer true.

8.2. Puddle World

We ran our system on a fixed Puddle World map of size 50×50 . In our setup the system dynamics are deterministic, our main goal being to show that our agent is able to find appropriate actions amongst a very large set (up to more than one million). To begin with we note that in the simple case with two actions, $n = 1$ in Figure (4) it is difficult to find a stable policy. We believe that this is due to a large number of states producing the same observation, which makes a high-frequency policy more difficult to learn. As the plans get longer, the policies get significantly better. The best possible score, without puddles, is 150 (50+50 steps of -1, and a final score of 250).

Figure (5) demonstrates performance on a 20-step plan

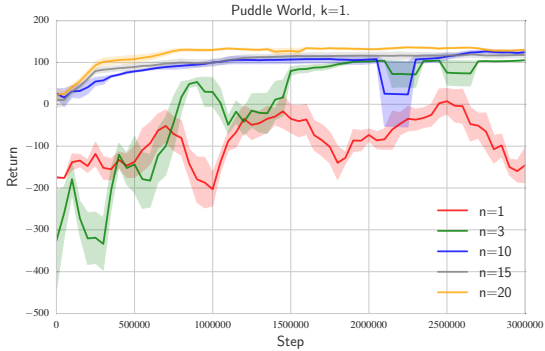


Figure 4. Agent performance for various lengths of plan, a plan of $n = 20$ corresponds to $2^{20} = 1,048,576$ actions. The agent is able to learn faster with longer plan lengths. $k = 1$ and ‘slow’ FLANN settings are used.

Puddle World with the number of neighbors $k = 1$ and $k = 52428$, or 5% of actions. In this figure $k = |\mathcal{A}|$ is absent as it failed to arrive to the first evaluation step. We can see that in this task we are finding a near optimal policy while never using the arg max pass of the policy. We see that even our most lossy FLANN setting with no re-ranking converges to an optimal policy in this task. As a large number of actions are equivalent in value, it is not surprising that even a very lossy approximate nearest neighbor search returns sufficiently pertinent actions for the task. Experiments on the recommender system in Section 8.3 show that this is not always this case.

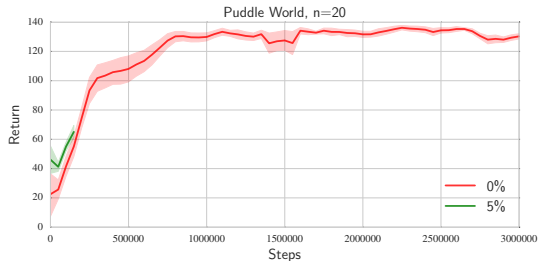


Figure 5. Agent performance for various percentages of k in a 20-step plan task in Puddle World with FLANN settings on ‘slow’.

Table 3 describes the median steps per second during training. In the case of Puddle World, we can see that we can get a speedup for equivalent performance of up to 1,250 times.

# Neighbors	Exact	Medium	Fast
1	4.8	119	125
0.5% – 5,242	0.2	0.2	0.2
100% – $1e6$	0.1	0.1	0.1

Table 2. Median steps/second as a function of k & FLANN settings.

8.3. Recommender Task

Experiments were run on 3 different recommender tasks involving 49 elements, 835 elements, and 13,138 elements. These tasks’ dynamics are quite irregular, with certain actions being good in many states, and certain states requiring a specific action rarely used elsewhere. This has the effect of rendering agents with $k = 1$ quite poor at this task. Additionally, although initial exploration methods were purely uniform random with an epsilon probability, to better simulate the reality of the running system — where state transitions are also heavily guided by user choice — we restricted our epsilon exploration to a likely subset of good actions provided to us by the simulator. This subset is only used to guide exploration; at each step the policy must still choose amongst the full set of actions if not exploring. Learning with uniform exploration converges, but in the larger tasks performance is typically 50% of that with guided exploration.

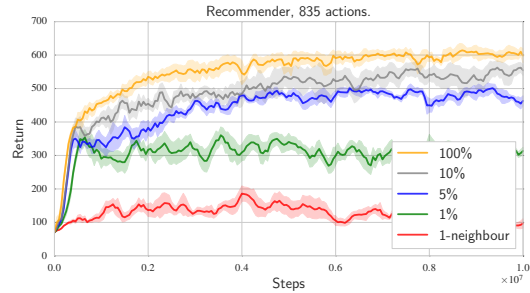


Figure 6. Performance on the 835-element recommender task for varying values of k , with exact nearest-neighbor lookup.

Figure 6 shows performance on the 835-element task using exact lookup for varying values of k as a percentage of the total number of actions. We can see a clear progression of performance as k is increased in this task. Although not displayed in the plot, these smaller action sizes have much less significant speedups, with $k = |\mathcal{A}|$ taking only twice as long as $k = 83$ (1%).

Results on the 13,138 element task are visualized in Figures (7) for varying values of k , and in Figure (8) with varying FLANN settings. Figure (7) shows performance for exact nearest- neighbor lookup and varying values of k . We note that the agent using all actions (in yellow) does not train as many steps due to slow training speed. It is training approximately 15 times slower in wall-time than the 1% agent.

Figure (8) shows performance for varying FLANN settings on this task with a fixed k at 5% of actions. We can quickly see both that lower-recall settings significantly impact the performance on this task.

Results on the 49-element task with both a 200-



Figure 7. Agent performance for various numbers of nearest neighbors on 13k recommender task. Training with $k = 1$ failed to learn.

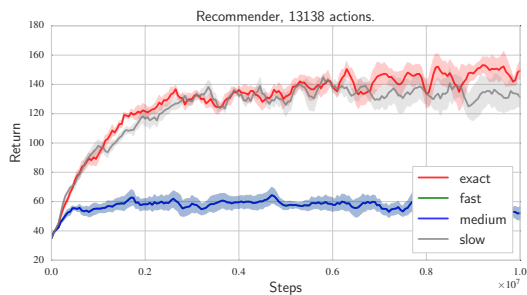


Figure 8. Agent performance for various FLANN settings on nearest-neighbor lookups on the 13k recommender task. In this case, fast and medium FLANN settings are equivalent. $k = 656$ (5%).

dimensional and a 20-dimensional representation are presented in Figure 9 using a fixed ‘slow’ setting of FLANN and varying values of k . We can observe that when using a small number of actions, a more compact representation of the action space can be beneficial for stabilizing convergence.

# Neighbors	Exact	Slow	Medium	Fast
1	31	50	69	68
1% – 131	23	37	37	37
5% – 656	10	13	12	14
10% – 1,313	7	7.5	7.5	7
100% – 13,138	1.5	1.6	1.5	1.4

Table 3. Median steps/second as a function of k & FLANN settings on the 13k recommender task.

Results on this series of tasks suggests that our approach can scale to real-world MDPs with large number of actions, but exploration will remain an issue if the agent needs to learn from scratch. Fortunately this is generally not the case, and either a domain-specific system provides a good starting state and action distribution, or the system’s dynamics constrain transitions to a reasonable subset of actions for a given states.

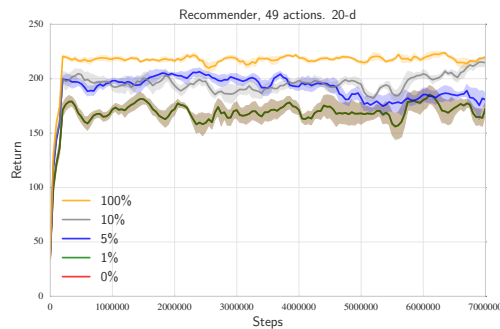
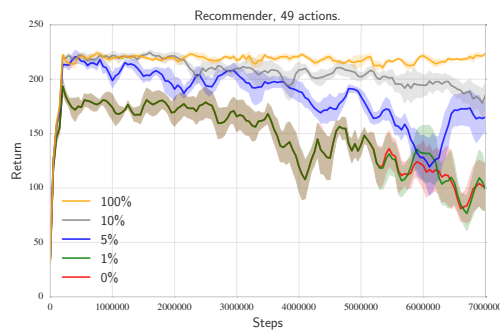


Figure 9. Recommender task with 49 actions using 200 dimensional action representation (left) and 20-dimensional action representations (right), for varying values of k and fixed FLANN setting of ‘slow’. The figure intends to show general behavior and not detailed values.

9. Conclusion

In this paper we introduce a new policy architecture able to efficiently learn and act in large discrete action spaces. We describe how this architecture can be trained using DDPG and demonstrate good performance on a series of tasks with a range from tens to one million discrete actions.

Architectures of this type give the policy the ability to generalize over the set of actions with sub-linear complexity relative to the number of actions. We demonstrate how considering only a subset of the full set of actions is sufficient in many tasks and provides significant speedups. Additionally, we demonstrate that an approximate approach to the nearest-neighbor lookup can be achieved while often impacting performance only slightly.

Future work in this direction would allow the action representations to be learned during training, thus allowing for actions poorly placed in the embedding space to be moved to more appropriate parts of the space. We also intend to investigate the application of these methods to a wider range of real-world control problems.

References

- Dietterich, Thomas G. and Bakiri, Ghulum. Solving multiclass learning problems via error-correcting output codes. *Journal of artificial intelligence research*, pp. 263–286, 1995.
- Dulac-Arnold, Gabriel, Denoyer, Ludovic, Preux, Philippe, and Gallinari, Patrick. Fast reinforcement learning with large action sets using error-correcting output codes for mdp factorization. In *Machine Learning and Knowledge Discovery in Databases*, pp. 180–194. Springer, 2012.
- Hafner, Roland and Riedmiller, Martin. Reinforcement learning in feedback control. *Machine learning*, 84(1-2):137–169, 2011.
- He, Ji, Chen, Jianshu, He, Xiaodong, Gao, Jianfeng, Li, Lihong, Deng, Li, and Ostendorf, Mari. Deep reinforcement learning with an unbounded action space. *arXiv preprint arXiv:1511.04636*, 2015.
- Lagoudakis, Michail and Parr, Ronald. Reinforcement learning as classification: Leveraging modern classifiers. In *ICML*, volume 3, pp. 424–431, 2003.
- Lillicrap, Timothy P, Hunt, Jonathan J, Pritzel, Alexander, Heess, Nicolas, Erez, Tom, Tassa, Yuval, Silver, David, and Wierstra, Daan. Continuous control with deep reinforcement learning. *arXiv preprint arXiv:1509.02971*, 2015.
- Lin, Long-Ji. Self-improving reactive agents based on reinforcement learning, planning and teaching. *Machine learning*, 8(3-4):293–321, 1992.
- Mnih, Volodymyr, Kavukcuoglu, Koray, Silver, David, Rusu, Andrei A, Veness, Joel, Bellemaire, Marc G, Graves, Alex, Riedmiller, Martin, Fidjeland, Andreas K, Ostrovski, Georg, et al. Human-level control through deep reinforcement learning. *Nature*, 518(7540):529–533, 2015.
- Muja, Marius and Lowe, David G. Scalable nearest neighbor algorithms for high dimensional data. *Pattern Analysis and Machine Intelligence, IEEE Transactions on*, 36, 2014.
- Pazis, Jason and Parr, Ron. Generalized value functions for large action sets. In *Proceedings of the 28th International Conference on Machine Learning (ICML-11)*, pp. 1185–1192, 2011.
- Prokhorov, Danil V, Wunsch, Donald C, et al. Adaptive critic designs. *Neural Networks, IEEE Transactions on*, 8(5):997–1007, 1997.
- Silver, David, Lever, Guy, Heess, Nicolas, Degris, Thomas, Wierstra, Daan, and Riedmiller, Martin. Deterministic policy gradient algorithms. In *Proceedings of The 31st International Conference on Machine Learning*, pp. 387–395, 2014.
- Sunehag, Peter, Evans, Richard, Dulac-Arnold, Gabriel, Zwols, Yori, Visentin, Daniel, and Coppin, Ben. Deep reinforcement learning with attention for slate markov decision processes with high-dimensional states and actions. *arXiv preprint arXiv:1512.01124*, 2015.
- Sutton, Richard S and Barto, Andrew G. *Reinforcement learning: An introduction*, volume 1. MIT press Cambridge, 1998.
- Todorov, Emanuel, Erez, Tom, and Tassa, Yuval. Mujoco: A physics engine for model-based control. In *Intelligent Robots and Systems (IROS), 2012 IEEE/RSJ International Conference on*, pp. 5026–5033. IEEE, 2012.
- Van Hasselt, Hado, Wiering, Marco, et al. Using continuous action spaces to solve discrete problems. In *Neural Networks, 2009. IJCNN 2009. International Joint Conference on*, pp. 1149–1156. IEEE, 2009.

Appendices

A. Detailed Wolpertinger Algorithm

Algorithm 2 describes the full DDPG algorithm with the notation used in our paper, as well as the distinctions between actions from \mathcal{A} and prototype actions.

The critic is trained from samples stored in a replay buffer. These samples are generated on lines 9 and 10 of Algorithm 2. The action \mathbf{a}_t is sampled from the full Wolpertinger policy π_θ on line 9. This action is then applied on the environment on line 10 and the resulting reward and subsequent state are stored along with the applied action in the replay buffer on line 11.

On line 12, a random transition is sampled from the replay buffer, and line 13 performs Q-learning by applying a Bellman backup on Q_{θ^Q} , using the target network’s weights for the target Q. Note the target action is generated by the full policy π_θ and not simply f_{θ^π} .

The actor is then trained on line 15 by following the policy gradient:

$$\begin{aligned} \nabla_\theta f_{\theta^\pi} &\approx \mathbb{E}_{f'} [\nabla_{\theta^\pi} Q_{\theta^Q}(\mathbf{s}, \hat{\mathbf{a}})|_{\hat{\mathbf{a}}=f_{\theta^\pi}(\mathbf{s})}] \\ &= \mathbb{E}_{f'} [\nabla_{\hat{\mathbf{a}}} Q_{\theta^Q}(\mathbf{s}, f_{\theta^\pi}(\mathbf{s})) \cdot \nabla_{\theta^\pi} f_{\theta^\pi}(\mathbf{s})]. \end{aligned}$$

Algorithm 2 Wolpertinger Training with DDPG

- 1: Randomly initialize critic network Q_{θ^Q} and actor f_{θ^π} with weights θ^Q and θ^π .
- 2: Initialize target network $Q_{\theta^{Q'}}$ and $f_{\theta^{\pi'}}$ with weights $\theta^{Q'} \leftarrow \theta^Q, \theta^{\pi'} \leftarrow \theta^\pi$
- 3: Initialize g 's dictionary of actions with elements of \mathcal{A}
- 4: Initialize replay buffer B
- 5: **for** episode = 1, M **do**
- 6: Initialize a random process \mathcal{N} for action exploration
- 7: Receive initial observation state \mathbf{s}_1
- 8: **for** $t = 1, T$ **do**
- 9: Select action $\mathbf{a}_t = \pi_\theta(\mathbf{s}_t)$ according to the current policy and exploration method
- 10: Execute action \mathbf{a}_t and observe reward r_t and new state \mathbf{s}_{t+1}
- 11: Store transition $(\mathbf{s}_t, \mathbf{a}_t, r_t, \mathbf{s}_{t+1})$ in B
- 12: Sample a random minibatch of N transitions $(\mathbf{s}_i, \mathbf{a}_i, r_i, \mathbf{s}_{i+1})$ from B
- 13: Set $y_i = r_i + \gamma \cdot Q_{\theta^{Q'}}(\mathbf{s}_{i+1}, \pi_{\theta'}(\mathbf{s}_{i+1}))$
- 14: Update the critic by minimizing the loss:
 $L(\theta^Q) = \frac{1}{N} \sum_i [y_i - Q_{\theta^Q}(\mathbf{s}_i, \mathbf{a}_i)]^2$
- 15: Update the actor using the sampled gradient:

$$\begin{aligned} \nabla_{\theta^\pi} f_{\theta^\pi} |_{\mathbf{s}_i} &\approx \\ \frac{1}{N} \sum_i \nabla_{\mathbf{a}} Q_{\theta^Q}(\mathbf{s}, \hat{\mathbf{a}}) |_{\hat{\mathbf{a}}=f_{\theta^\pi}(\mathbf{s}_i)} \cdot \nabla_{\theta^\pi} f_{\theta^\pi}(\mathbf{s}) |_{\mathbf{s}_i} \end{aligned}$$

- 16: Update the target networks:

$$\begin{aligned} \theta^{Q'} &\leftarrow \tau \theta^{Q'} + (1 - \tau) \theta^Q \\ \theta^{\pi'} &\leftarrow \tau \theta^{\pi'} + (1 - \tau) \theta^\pi \end{aligned}$$

- 17: **end for**
- 18: **end for**

Actions stored in the replay buffer are generated by π_{θ^π} , but the policy gradient $\nabla_{\hat{\mathbf{a}}} Q_{\theta^Q}(\mathbf{s}, \hat{\mathbf{a}})$ is taken at $\hat{\mathbf{a}} = f_{\theta^\pi}(\mathbf{s})$. This allows the learning algorithm to leverage otherwise ignored information of which action was actually executed for training the critic, while taking the policy gradient at the actual output of f_{θ^π} .

B. Proof of Lemma 1

Proof. Without loss of generality we can assume $Q(s, a) = \frac{1}{2}$, $b = \frac{1}{2}$ and replace c with $c' = \frac{c}{2b}$, resulting in an affine transformation of the original setting. We undo this transformation at the end of this proof to obtain the general result.

There is a p probability that an action is ‘bad’ and has value $-c'$. If it is not bad, the distribution of the value of the action is uniform in $[Q(s, a) - b, Q'(s, a) + b] = [0, 1]$. This

implies that the cumulative distribution function (CDF) for the value of an action $i \in \{1, \dots, k\}$ is

$$F(x; s, i) = \begin{cases} 0 & \text{for } x < -c \\ p & \text{for } x \in [-c, 0) \\ p + (1 - p)x & \text{for } x \in [0, 1] \\ 1 & \text{for } x > 1. \end{cases}$$

If we select k such actions, the CDF of the maximum of these actions equals the product of the individual CDFs, because the probability that the maximum value is smaller than some given x is equal to the probability that all of the values is smaller than x , so that the cumulative distribution function for

$$\begin{aligned} F_{\max}(x; s, a) &= P\left(\max_{i \in \{1, \dots, k\}} Q(s, i) \leq x\right) \\ &= \prod_{i \in \{1, \dots, k\}} P(Q(s, i) \leq x) \\ &= \prod_{i \in \{1, \dots, k\}} F(x; s, i) \\ &= F(x; s, 1)^k, \end{aligned}$$

where the last step is due to the assumption that the distribution is equal for all k closest actions (it is straightforward to extend this result by making other assumptions, e.g., about how the distribution depends on distance to the selected action). The CDF of the maximum is therefore given by

$$F_{\max}(x; s, a) = \begin{cases} 0 & \text{for } x < -c' \\ p^k & \text{for } x \in [-c', 0) \\ (p + (1 - p)x)^k & \text{for } x \in [0, 1] \\ 1 & \text{for } x > 1. \end{cases}$$

Now we can determine the desired expected value as

$$\begin{aligned} &\mathbb{E}\left[\max_{i \in \{1, \dots, k\}} Q(s, i)\right] \\ &= \int_{-\infty}^{\infty} x \, dF_{\max}(x; s, a) \\ &= p^k \left(\frac{1}{2} - c'\right) + \int_0^1 x \, dF_{\max}(x; s, a) \\ &= p^k \left(\frac{1}{2} - c'\right) + [xF_{\max}(x; s, a)]_0^1 - \int_0^1 F_{\max}(x; s, a) \, dx \\ &= p^k \left(\frac{1}{2} - c'\right) + 1 - \int_0^1 (p + (1 - p)x)^k \, dx \\ &= p^k \left(\frac{1}{2} - c'\right) + 1 - \left[\frac{1}{1 - p} \frac{1}{k + 1} (p + (1 - p)x)^{k+1}\right]_0^1 \\ &= p^k \left(\frac{1}{2} - c'\right) + 1 - \left(\frac{1}{1 - p} \frac{1}{k + 1} - \frac{1}{1 - p} \frac{1}{k + 1} p^{k+1}\right) \\ &= 1 + p^k \left(\frac{1}{2} - c'\right) - \frac{1}{k + 1} \frac{1 - p^{k+1}}{1 - p}, \end{aligned}$$

where we have used $\int_0^1 x \, d\mu(x) = \int_0^1 1 - \mu(x) \, dx$, which can be proved by integration by parts. We can scale back to the arbitrary original scale by subtracting $1/2$, multiplying by $2b$ and then adding $Q(s, a)$ back in, yielding

$$\begin{aligned}
 & \mathbb{E} \left[\max_{i \in \{1, \dots, k\}} Q(s, i) \right] \\
 &= Q(s, a) + 2b \left(1 + p^k \left(\frac{1}{2} - c' \right) - \frac{1}{k+1} \frac{1-p^{k+1}}{1-p} - \frac{1}{2} \right) \\
 &= Q(s, a) + b + p^k b - p^k c - \frac{2b}{k+1} \frac{1-p^{k+1}}{1-p} \\
 &= Q(s, a) + b - p^k c - b \left(\frac{2}{k+1} \frac{1-p^{k+1}}{1-p} - p^k \right) \quad \square
 \end{aligned}$$